Colloids and Surfaces B: Biointerfaces 217 (2022) 112683

Contents lists available at ScienceDirect

Colloids and Surfaces B: Biointerfaces

journal homepage: www.elsevier.com/locate/colsurfb

Effect of solvent and additives on the electrospinnability of BSA solutions

Javier Garcia [a], Manuel Felix [b,*], Felipe Cordobés [b], Antonio Guerrero [b]

[a] Facultad de Química, Universidad de Sevilla, Spain
[b] Escuela Politécnica Superior, Universidad de Sevilla, Spain

ARTICLE INFO

Keywords:
Biomaterials
Nanofibers
Electrospinning
BSA
Surface tension
Viscosity

ABSTRACT

Electrospun nanofibrous membranes have attracted the interest of the scientific community over the past decades due to their unique properties (e.g., high surface area, enzyme encapsulation high efficiency in filtering). Among the most promising membranes are those derived from natural polymers, which are not based on fossil fuels and most of them are highly biocompatible. In this regard, this study is focused on the development and characterization of electrospun nanofibrous membranes of bovine serum albumin (BSA) with potential applications in several fields, from tissue engineering to advanced filtering. Although the globular structure of BSA hinders the generation of nanofibers, some previous studies have succeeded in its electrospinning. However, they made use of either toxic reagents or co-electrospinning with synthetic polymers, which resulted in poorer biocompatibility. To prevent this, the present study explores the impact of non-hazardous reagents on the formation of BSA nanofibers. As a result, it was observed that the addition of ethanol (EtOH) in the solvent mixture and the thermal denaturation of BSA favored the electrospraying of nanoparticles (~ 300 nm). It was also noticed that the presence of hydroxypropyl methylcellulose (HPMC) favors the formation of nanofibers (~ 60 nm). However, bead formation was found in these membranes. This work contributes to clarifying the influence of solvents and surfactants when proteins are electrospun, enabling the manufacture of bio-based nanofibrous mats with applications in different fields (e.g., filtering, biomaterials, active packaging).

1. Introduction

The scientific community have shown a growing interest in the development and use of polymer-based nanofibers [1]. Nanofibers are ultra-fine solid fibers exhibiting extraordinary properties due to their very small diameters (which typically range from a few nanometers to 5 μm [2]. Thus, their large surface area per unit mass and small pore size generate a wide range of applications in several fields, such as tissue engineering, filter production, biosensors development, optoelectronic devices and even in catalysis [3–7]. Nanofibers can be made of synthetic or natural polymers and there are diverse ways of developing them [8–10]. Among the most widespread methods, electrospinning, chemical vapor deposition and the template method are among the most used [11]. Indeed, electrospinning is considered the most promising method since it offers several advantages, such as easy installation, versatility, efficiency and cost-effectiveness [12,13].

Electrospinning is affected by a broad range of factors, including experimental (voltage, distance needle-collector, type of collector), environmental (humidity and temperature) and solution conditions (viscosity, pH, conductivity, surface tension) [14,15]. Among them, viscosity and surface tension are key parameters in the process [16]. Viscosity increases with polymer concentration and with its molecular weight. It also keeps a close relationship with the molecular structure, being enhanced by the formation of long chains that are stacked with high degrees of crystallinity, forming entanglements [17]. High viscosity values could lead to the formation of helix-shaped fibers and may even fail to flow through the needle [18]. When the surface tension is excessively high, spheroids might appear on the fibers [19,20]. Besides, low viscosities or high surface tensions may result in the formation of beads in the nanofibers or even in the formation of nano or microparticles instead of nanofibers. In such a case, it would no longer make sense to talk about electrospinning when referring to this technique. Instead, nanoparticles electrospraying would take place [21].

In this balance between the different factors involved in the process, the solvent exerts a crucial role [22]. The solvent must be volatile enough whereby it evaporates during the process and must be able to properly dissolve the polymer [23]. Solubility is strongly dependent on the physical interactions between the polymer molecules and the

* Corresponding author.
E-mail address: mfelix@us.es (M. Felix).

https://doi.org/10.1016/j.colsurfb.2022.112683
Received 9 May 2022; Received in revised form 27 June 2022; Accepted 29 June 2022
Available online 3 July 2022

solvent. It will increase as the solvent ability to generate electrostatic interactions via hydrogen bonding, polar forces or London dispersion forces with the polymer increase [24,25]. In systems based on natural polymers, the choice of solvent and the addition of reagents which may affect the above-mentioned properties may play an active role in the polymer solubility and in achieving suitable properties for electrospinning [26]. Some solvents, such as ethanol and certain acids, are also considered to be denaturing agents [27,28]. The structural changes caused by the solvent would help to solubilize the polymer and, in some cases, may increase the interactions between polymer chains, leading to an increase in viscosity [29]. These changes could also be enhanced by changes in pH value, thermal denaturation, conductivity alterations or the addition of denaturing agents [30].

Synthetic polymers are cost-effective and provide great versatility in terms of mechanical and optical properties, biodegradability, etc of the final mats produced [31]. However, they are sourced directly or indirectly from fossil fuels. In recent years, due to society's growing awareness of the use of such raw materials, several attempts have been made to replicate this technique using polymers derived either from recycled synthetic polymers [32,33] or from natural sources such as bacterial cultures or crustacean shells (i.e., biopolymers) [8,34,35]. Some carbohydrates have been reported to be suitable for electrospinning processing, as is the case of chitosan and cellulose acetate [36,37]. However, these biopolymers have limited solubility. An alternative is carboxymethyl cellulose, which is a biocompatible derivative of cellulose, soluble in a wide variety of pH values [38]. The electrospinnability of globular proteins is limited. However, the morphology and the mechanical properties of the mats produced can be modulated by modifying the tertiary structure of proteins (i.e., protein conformation, protein aggregation, and consequently the inter/intramolecular bonds) [39]. Moreover, the protein threshold concentration (related in many cases to solution viscosity) is related to the molecular weight of proteins, where the formation of disulfide bonds must be considered [40]. Mendes et al. [41] indicated that proteins must be at least partially unfolded when they are electrospun. The solvent, heat, or additives can lead to these changes in protein conformation.

Biopolymers usually have advantageous properties when used in health and food applications, since they often exhibit antibacterial properties and are generally biocompatible and biodegradable [42,43]. Although a wide variety of synthetic polymers have been successfully electrospun to date, only a few authors have published papers concerning the electrospinning of globular proteins [39,41,44].

The aim of this work has been the development and characterization of Bovine Serum Albumin (BSA)-based nanofibrous membranes processed by electrospinning. To this end, different ratios H_2O:EtOH (100:0, 80:20 and 70:30) were evaluated at the same time as some additives with effect on protein morphology (β-mercaptoethanol, ethanol, SDS and Tween-20) [45–48]. Interfacial tension, conductivity, and viscosity measurements were carried out to analyze the effect of the solution parameters on the final mats, whereas the mats were evaluated by SEM microscopy. Thus, this work is focused on the effect of the properties of the precursor solution over the final features of the resulting membranes and the effect of the addition of surfactants and other substances over the whole process.

2. Materials and methods

2.1. Materials

Bovine Serum Albumin (BSA), Hydrochloric acid (HCl), Sodium Hydroxide (NaOH) and Sodium Chloride (NaCl) were purchased from Panreac AppliChem (Barcelona, Spain), whereas Sodium Azide (NaN_3), Sodium Dodecyl Sulfate (SDS), β-Mercaptoethanol (β-ME), Hydroxypropyl Methylcellulose (HPMC) were purchased from Sigma & Aldrich (Saint Louis, USA).

2.2. Methods

2.2.1. Preparation and electrospinning of solutions

Different series of samples were prepared at pH 7.0 by the addition of NaOH and HCl. These values were controlled by using a MicropH 2001 (Crison Instruments, Barcelona, Spain). The following additives were studied: (i) the effect of SDS (0.1 wt%, 1 wt%) and β-ME (0.5 M) was evaluated for 10 wt% BSA aqueous dispersions; (ii) the effect of EtOH (H_2O:EtOH 80:20, 70:30) was evaluated for systems containing 10 wt% BSA. (iii) the effect of HPMC (1.5, 2, 2.5, 3 and 3.5 wt%) was studied for 10 wt% BSA in EtOH:H_2O (20:80). Moreover, different reagents (SDS 0.1 wt%, Tween-20 0.006 mM, NaCl 10^{-3} M) were added to these samples. The solubility of BSA decreased when ethanol was added, consequently, 20 and 30 wt% EtOH was evaluated (ratios 80:20 and 70:30, respectively). The NaCl concentration was set to raise the conductivity by an order of magnitude [49,50]. SDS and Tween-20 (ionic and non-ionic surfactants, respectively) were added to reduce the surface tension of the BSA solutions. The lower SDS concentration was selected since it seemed to facilitate BSA electrospinning instead of promoting protein denaturation [51,52]. Moreover, the Tween-20 concentration (0.006 mM) was selected because it facilitates HPMC electrospinning [53].

The solutions prepared were processed in a Fluidnatek LE-50 (Bioinicia, Valencia, Spain). The solutions were pumped through a 0.5 mm diameter needle at a constant flow rate of 0.4 mL/h. The needle was placed 13.5 cm from the collector and the voltage was settled at 16–30 kV. Samples were processed at 25 °C and 30% humidity.

2.2.2. Physicochemical characterization of biopolymer solutions

Surface tension was determined with a Sigma 7^{01} Tensiometer and conductivity using a Crison EC-Meter Basic 30 + (Crison Instruments, Barcelona, Spain), while density was obtained using a Crison EC-Meter Basic 30 + (Crison Instruments, Barcelona, Spain).

The viscosity of aqueous solutions was determined using an Ubbelohde viscometer at low viscosity solutions ($< 1{\cdot}10^{-3}$ Pa·s). Higher viscosities of aqueous solutions were characterized using the AR-2000 rheometer (TA-Instruments, Massachusetts, USA). The gelation of BSA solutions was assessed by the evolution of viscoelastic moduli (G' and G'') as a function of time, at a heating rate of 5 °C/min. The solvent tramp accessory was used to avoid solvent evaporation during heating. Steady-state flow curves (from 0.1 to 100 s^{-1}) were performed to systems containing HPMC. All rheological measurements were performed within the linear viscoelastic range, the tool used was serrated parallel plates (60 mm) at 1 mm gap.

2.2.3. Scanning electron microscopy (SEM)

Micrographs of the fibrous mats were obtained by using the Zeiss EVO LS15 electron microscope (Jena, Germany). The samples were sputtered with an Au-Pd coating in a vacuum chamber at $9{\cdot}10^{-3}$ bar to achieve a layer thickness of about 12 nm. Once coated, samples were placed in the holder of the microscope. Images were obtained from 2 to 5 mm working distance from the detector. The acceleration voltage selected was 10 kV. The nanofiber diameter was studied using the ImageJ software (Bethesda, USA).

2.2.4. Mechanical characterization

The mechanical spectrum of the membrane obtained at 10 wt% BSA and 3 wt% HPMC was obtained by frequency sweep test (from 0.01 and 10 Hz). The frequency sweep tests were performed in tension mode within the linear viscoelastic (LVE) range, which was determined by an amplitude sweep test performed at 1 Hz. Stress-strain curves were obtained by continuous deformation tests at constant deformation rate (1 mm/min). These measurements were performed using rectangular probes (10x30mm) at room temperature by a DMA850 (TA instruments, MA, USA).

2.3. Statistical analyses

At least three replicates of each measurement were carried out. Statistical analyses were performed using one-way analysis of variance (ANOVA) test ($\rho < 0.05$). These tests were performed using the Microsoft Excel software (Raymond, USA). Standard deviations (SD) from some selected parameters were calculated.

3. Results and discussion

3.1. Effects of denaturing agents

Table 1 shows the values for surface tension, conductivity, density and dynamic viscosity for the solutions containing 10 wt% BSA and additives (β-ME and SDS). The effect of BSA concentration was also evaluated (results not shown), however lower BSA concentrations (5 wt %) did not perform properly in the electrospinning processing, whereas higher BSA concentrations (12 wt%) led to solubility problems. The β-ME and SDS additives were used since they were previously related to protein denaturation by a different mechanism. β-ME is able to reduce disulfide bonds, whereas SDS disrupts electrostatic interactions of proteins [54,55].

Table 1 indicates that the surface tension of the solutions decreases with the SDS. This result can be expected since SDS has an amphiphilic character, at the same time as SDS is above the critical micelle concentration [56]. Small concentrations of SDS in protein/SDS mixtures have been reported to increase protein stability in water. Moreover, when SDS concentration becomes sufficiently large, these interactions become stronger and lead to protein unfolding [57]. The protein conformation changes are confirmed by the changes in surface tension observed in Table 1. Solution conductivity increased when SDS was added, which can be expected since SDS is an ionic surfactant, whereas density values increased with solute concentration, however, no remarkable changes were observed.

Previous research works reported the formation of nanofibrous mats at surface tension values ranging from 55 mN/m to 30 mN/m [19,52,58,59], being all the solutions prepared within this range. The conductivity results did not follow any trend due to the addition of different amounts of HCl and NaOH to set the pH value at 7.0. According to some authors [53,58,60], there is an optimal range of conductivities for the electrospinning of solutions. This range would roughly span from 5 μS/cm to 2000 μS/cm, leaving some of the solutions analyzed in this work above this range. β-ME and SDS influenced the solution conductivity. The effect of SDS could be attributed to its ionic character, the increase in conductivity found after the β-ME addition must be attributed to conformational changes in the BSA protein. The dynamic viscosity of the solutions is also key for the performance of biopolymers solutions by electrospinning processing. The dynamic viscosity of 10 wt% BSA solution was 1.907 ± 0.007 mPa·s, which was significantly lower than the suitable range experimentally determined (from 0.1 to 50 Pa·s) [61–63]. This low viscosity value would be caused by the fact that the BSA molecules do not interact with each other through entanglements due to their globular structure and, so that, the viscosity of the solution is mainly driven by the viscosity of the solvent, water.

Supplementary Fig. 1 shows the micrographs obtained for these systems reported in Table 1. All the micrographs have a magnification of 10,000 X, except for Fig. 1A and 1D, which were taken at 50 X. No nanofibrous mats were obtained. Instead, some spherical and spheroidal particles were developed for protein-based mats processed by electrospinning in presence of additives (β-ME 0.5 M; SDS 0.1 wt%; SDS 1 wt%; SDS 1 wt%, β-ME 0.5 M, Figs. 1B, 1C, 1E and 1F), whereas the formation of a membrane with no network-like structure took place (Fig. 1A, no additives; and 1D, SDS 0.1 wt%, β-ME 0.5 M). The pore diameter of these membranes was 100 ± 40 μm (Supplementary Fig. 1 A) and 60 ± 30 μm (Supplementary Fig. 1D). It seems that there is not a clear correlation between the observed.

microstructures and the concentrations of and β-ME. The solutions electrospun in this series of tests did not result in the formation of nanofibers. These results may be mainly due to the low viscosity of these dissolutions. Viscosity is one of the most dominating parameters in electrospinning [19]. So that, low viscosity values result in jet breakage, which would disaggregate into particles of different sizes [17]. Thus, these reagents would not enhance the electrospinning of nanofibers under the processing conditions followed.

3.2. Effect of EtOH in solvent

Table 2 shows the physicochemical properties (surface tension, conductivity, density and dynamic viscosity) obtained for BSA-based solutions dissolved in EtOH:H_2O (80:20 or 70:30) with or without additives (SDS and/or β-ME). The results reported for the effect of solvent (except for viscosity) are within the range for electrospinning given by the literature [17,53,58,60–64]. Although viscosity of the dissolutions in Table 2 increases with BSA concentration, this dependence is weak and the viscosity remains two orders of magnitude below the minimum reported in the literature.

To achieve the required viscosities, the impact of thermal denaturation of BSA on nanofiber formation was also explored. Firstly, a temperature ramp was performed to determine the impact that the presence of ethanol has on the possible denaturation. Fig. 1 shows the evolution

Table 1
Properties (surface tension, conductivity, density and dynamic viscosity) of the solutions containing 10 wt% BSA and different amounts of β-Me and SDS.

Sample	Additive	Surface tension (mN/m)	Conductivity (μS/cm)	Density (kg/m^3)
10% BSA	No additive	50 ± 1	1080 ± 180	1018.9 ± 1.3
	0.5 M β-ME	–	1830 ± 130	1019.3 ± 1.1
	0.1 wt% SDS	46 ± 1	2210 ± 150	1021.0 ± 0.4
	0.1 wt% SDS + 0.5 M β-ME	–	2410 ± 120	1022.1 ± 0.9
	1 wt% SDS	41 ± 1	2530 ± 110	1024.6 ± 1.2
	1 wt% SDS + 0.5 M β-ME	–	2750 ± 150	1024.8 ± 0.6

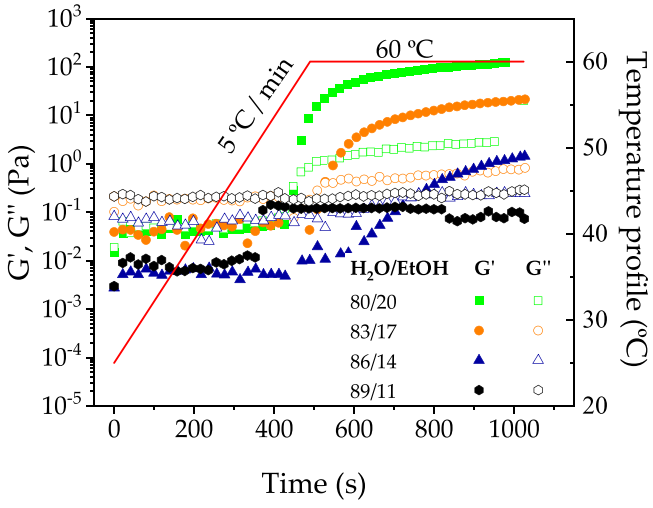

Fig. 1. Dependence of viscoelastic moduli with temperature for samples with different H_2O:EtOH ratios: 80:20, 83:17, 86:14 and 89:11.

Table 2
Surface tension, conductivity, density, and dynamic viscosity obtained for the solutions containing different amounts of BSA, ethanol β-ME.

H_2O: EtOH Ratio	Sample	Surface tension (mN/m)	Conductivity (μS/cm)	Density (kg/m^3)	Dynamic viscosity (mPa·s)
80:20	10 wt% BSA	35 ± 1	644 ± 80	997.5 ± 1.2	3.068 ± 0.004
80:20	10 wt% BSA β-ME 0.1 M	–	759 ± 60	998.0 ± 0.9	–
80:20	15 wt% BSA	32 ± 1	1109 ± 130	1007.6 ± 1.4	3.753 ± 0.006
70:30	10 wt% BSA	31 ± 1	489 ± 70	960.3 ± 0.7	3.307 ± 0.006

Table 3
Conductivity and density of the solutions containing 10 wt% BSA and different amounts of HPMC and reagents (Tween-20, SDS, NaCl).

Sample		Conductivity (μS/cm)	Density (kg/m^3)
10 wt% BSA	1.5 wt% HPMC	610 ± 60	998 ± 13
	2 wt% HPMC	499 ± 70	999 ± 10
	2.5 wt% HPMC	570 ± 40	1001 ± 15
	3 wt% HPMC	520 ± 30	1005 ± 16
	3.5 wt% HPMC	560 ± 80	1006 ± 11
	3 wt% HPMC + 0.006 mM Tween-20	630 ± 70	1004 ± 17
	3 wt% HPMC + 0.1 wt% SDS +	1820 ± 90	1006 ± 12
	3 wt% HPMC 15 mM NaCl	1520 ± 50	1012 ± 10
No BSA	1.5 wt% HPMC	110 ± 10	991 ± 10

viscoelastic moduli (G' and G'') with temperature.

Samples containing 10 wt% BSA were prepared in systems with different ratios of H_2O:EtOH (80:20, 83:17, 86:14 and 89:11). As a consequence of the heat treatment, the elastic modulus (G') undergoes a strong increase at around 60 °C. A significant increase in G' would be associated with the denaturation and crosslinking of BSA, enhancing its elastic behavior (which is known as BSA gelation). This effect is enhanced for higher ethanol concentrations. These results are in line with the available information in the literature, which discusses the denaturation of BSA due to temperature [65] and how ethanol favors its gelation [66]. The loss modulus (G"), which on the other hand is related to the viscous component in viscoelastic systems, remains constant. Moreover, although η * may not match with the dynamic viscosity of the systems, there is a proportional correlation between these two values [67]. Thus, it is possible to calculate the complex viscosity (η*) from their moduli G' and G", and so that the system with the highest moduli will be the one with the highest η*. Finally, the solution with BSA 10 wt % of and H_2O:EtOH (80:20), previously heated up to 60 °C, was electrospun as well as the rest of the samples commented in Table 2.

Supplementary Fig. 2 shows the micrographs obtained from the electrospinning of the systems containing EtOH, additives, and heated (60 °C). Regarding the Supplementary Fig. 2A-D, it seems that the denaturation of BSA induced by the presence of EtOH favors the electrosprying of nanoparticles rather than the formation of nanofibers. Nanoparticles obtained from the different tests ranged from 100 nm to 900 nm in diameter, and there were no major differences between samples. Given what is observed in Supplementary Fig. 2E, it also seems that viscosity is not the only impediment to the formation of nanofibers. The sample heated at 60 °C does not seem to reach a different microstructure from the rest of the samples despite a significant viscosity improvement. This might occur due to the formation of crosslinks upon thermal denaturation. These chemical bonds rigidize the structure of the polymeric network and would obstruct the movement between the chains, hindering the formation of nanofibers.

3.3. Effects of HPMC in the solvent system

BSA solutions were electrospun with HPMC to increase their viscosity. However, HPMC has been reported to interact with proteins, which can affect their functionality [68,69]. Moreover, HPMC is a polysaccharide derived from methylcellulose, which has been reported to favor the electrospinnability of protein solutions [38,53]. Thus, this polysaccharide would favor the presence of entanglements, which increase the viscosity of the solution. Its short lifetime.

allows movement between the polymeric chains, which could enhance the formation of nanofibers [20]. Thus, the network formed by the polymer chains could serve as structural support for BSA in the formation of nanofibers.

Table 3 lists the results of conductivity and density for solutions containing 10 wt% BSA and different amounts of HPMC (1.5, 2, 2.5, 3 and 3.5 wt%) and additives (Tween-20, SDS, NaCl).

Table 3 indicates that the concentration of HPMC does not have a significant effect on the conductivity of the samples, which can be attributed to the electrically neutral character of HPMC. Similarly, the addition of Tween-20 (non-ionic surfactant) does not affect the conductivity. However, SDS and NaCl increase the conductivity by an order of magnitude, as they introduce charges into the medium.

Supplementary Fig. 3 shows the flow curves for H_2O:EtOH solutions (80:20) containing 10 wt% BSA and HPMC. The flow behavior of the BSA-based solutions is typical of pseudoplastic materials, in which viscosity decreases with shear rate [70]. Moreover, the viscosity profile in that figure describes a plateau region at low shear rates (which is more evident at lower HPMC content), while at higher shear rates the viscosity decreases more rapidly (indicating stronger shear thinning behavior). The higher viscosity observed as the concentration of HPMC increases can be related to the fact that the HPMC provides a higher degree of entanglement, which makes fluid movement more difficult when the solution is under shear stresses [71]. The presence of BSA causes a slight drop in viscosity. As previously mentioned, the protein could be altering the network formed by the HPMC chains. Thus, the rheological response of these solutions is dominated by the HPMC, playing the BSA a marginal role in the bulk rheology of the solutions electrospun.

The effect exerted by the presence of two different surfactants on the viscosity of the system was also studied. As a result, it was obtained that the viscosity of the systems was slightly reduced after the addition of Tween-20, while this reduction became more sensitive in the presence of SDS. Unlike Tween-20, SDS is an ionic surfactant, which introduces new charges into the system. These charges could bind to BSA, or give rise to electrostatic repulsions, altering the net charge of the protein and thus causing more severe network disruption. This alteration would cause a drop in viscosity and elastic modulus of the solutions.

Note that the working conditions of the electrospinning experimental set-up would lead to a shear rate of c.a. 10 s^{-1} when the solution is flowing through the electrospinning needle. Attending to the results shown in Table 3, all the systems studied would be within the optimal range of viscosities for electrospinning (0.1–50 Pa-s [61–63]). However, it was impossible to electrospun the system with 3.5 wt% HPMC, as it did not flow through the needle.

The curves in Supplementary Fig. 3 fit the Williamson model for shear thinning behavior, in which viscosity depends on shear rate as shown in Eq. 1:

$$\eta = \frac{\eta_0}{1 + (k \cdot \dot{\gamma})^n} \quad (1)$$

where η (Pa·s) is the viscosity of the system at a given shear rate, η_0 (Pa·s) is the zero-shear rate viscosity, k (s) is the consistency, $\dot{\gamma}$ (s^{-1}) is the given shear rate and n is the flow index. The flow index ranges from 0 to 1, where 0 corresponds to a pure Newtonian behavior and 1, to a pure shear-thinning behavior.

Table 4 shows the values of n, k and η_0 for the samples in Supplementary Fig. 3. As shown in this table, n values increase with HPMC concentration. BSA solution behaves as a Newtonian fluid in the studied range [72]. So that, as the HPMC is added, its shear-thinning behavior would increasingly prevail, indicating that the rheological behavior of BSA/HPMC mixtures is dominated by HPMC. The prevalence of HPMC over BSA in the solutions is also confirmed by the η_0 values since it increased with HPMC concentration (from 2.89 ± 0.12–43.2 ± 0.4), and decreased with BSA (from 9.39 ± 0.16–2.89 ± 0.12).

Fig. 2 shows the micrographs of HPMC containing samples (1.5, 2, 2.5 and 3 wt%) and BSA (10 wt%) dissolved in H_2O:EtOH (80:20). The formation of nanofibers with beads can be observed in these micrographs, depending on the HPMC concentrations. Thus, the fiber diameter does not vary much between systems, remaining between 50 and 60 nm. The effect of HPMC concentration on fiber shape can be seen by comparing the results of the different systems.

Systems with lower HPMC concentration, and therefore less viscous, have larger and denser beads, which could be considered as nanoparticles interconnected through nanofibers. As the concentration of HPMC increases, beading decreases. This lower bead density could be due to the higher viscosity of the samples. Moreover, samples with lower viscosity values do not seem to provide sufficiently extensional viscosity to the jet to maintain proper stability during nanofiber formation, leading to higher bead formation [17].

It could also happen that the protein reduced the interactions between the solvent molecules and the polymer chains. In this scenario, BSA would tend to accumulate in beads, while HPMC would concentrate in the fibers. As the concentration of HPMC increases, the interactions between the polysaccharide chains and the solvent molecules would become more and more important, reducing beading. To test this hypothesis, EDX was performed on one of the samples (10 wt% BSA, 3 wt% HPMC). Nitrogen (N) content is related to BSA concentration (since it is the only N source) [73]. It was obtained a N content of 14 ± 2% in fibers and 21 ± 2% in beads. The presence of nitrogen in nanofibers is observed, confirming the co-electro-spinning between BSA and HPMC. BSA would be accommodated in the macromolecular lattice formed by the HPMC chains. However, a higher concentration of BSA is observed in beads, so even if co-electro-spinning occurs, BSA would disturb the network formed by the HPMC, reducing the interactions between the polysaccharide and the solvent molecules. This reduced interaction would make the surface tension forces in the jet predominate, leading to the formation of beads [17,20]. Thus, changes in beading for different HPMC concentrations would be caused by the combined effect of viscosity and destabilization on the HPMC network by BSA.

Fig. 3 shows additional micrographs carried out to understand the effect that the different components (BSA, Tween-20, SDS, NaCl) exert on the morphology of the nanofibers. Comparing Figs. 2D and 3A (10 wt % BSA 3 wt% HPMC and 10 wt% BSA 3 wt% HPMC Tween-20 0.006 mM) it can be seen how the addition of Tween-20 to the system causes beading to decrease. Based on this result, it seems that the system in Fig. 2D would have a high surface tension, which would favor the agglomeration of solvent molecules in the electrospinning jet [17].

The micrographs in Figs. 3B and 3C (10 wt% BSA 3 wt% HPMC 0.1 wt% SDS and 10 wt% BSA 3 wt% HPMC 15 mM NaCl), compared to that in Fig. 2D (10 wt% BSA 3 wt% HPMC), show how the presence of electrolytes hinders electrospinning of the system. In these figures, nanoparticle formation is favored over nanofiber formation. The charges added to the system would neutralize those of the BSA, causing the BSA to cause greater distortion of the polysaccharide chains and favoring nanoparticle formation. The charges would facilitate the gelation of the BSA into a rigid network, with crosslinking points, which would make electrospinning difficult [74]. The micrographs in Figs. 3B and 3C (10 wt% BSA 3 wt% HPMC 0.1 wt% SDS and 10 wt% BSA 3 wt% HPMC 15 mM NaCl), compared to that in Fig. 2D (10 wt% BSA 3 wt% HPMC), show how the presence of electrolytes hinders electrospinning of the system. In these figures, nanoparticle formation is favored over nanofiber formation.

Looking at Figs. 2B and 3D (BSA 10 wt%, HPMC 2 wt%, 13.5 cm; BSA 0 wt%, HPMC 2 wt%, 13.5 cm), it can also be seen how the presence of BSA alters the network formed by HPMC. Fig. 3D shows gray areas because part of the solvent did not dry on the way from the jet to the collector. The charges introduced by the BSA destabilize the jet and favor solvent removal [19,20], yet cause beading to appear. The electrospinning of BSA-based nanofibrous mats has been previously reported [4]. No beads were observed in these fibers, although they were co-electrospun with polyethylene oxide, a synthetic polymer.

Table 4
Zero-rate viscosity (η_0), rate index (n), and consistency (k) for the flow curves shown in Supplementary Fig. 3.

Sample		η_0 (Pa·s)	n	k (s)
10 wt% BSA	1.5 wt% HPMC	2.89 ± 0.12	0.65 ± 0.02	0.019 ± 0.005
	2 wt% HPMC	8.31 ± 0.08	0.73 ± 0.02	0.035 ± 0.002
	2.5 wt% HPMC	21.4 ± 0.1	0.75 ± 0.02	0.067 ± 0.004
	3 wt% HPMC	40.3 ± 0.2	0.74 ± 0.02	0.088 ± 0.007
	3.5 wt% HPMC	43.2 ± 0.4	0.74 ± 0.02	0.096 ± 0.005
	3 wt% HPMC + 0.006 mM Tween-20	40.1 ± 0.2	0.75 ± 0.02	0.087 ± 0.002
	3 wt% HPMC + 0.1 wt% SDS	30.30 ± 0.2	0.73 ± 0.02	0.080 ± 0.005
No BSA	1.5 wt% HPMC	9.39 ± 0.16	0.68 ± 0.02	0.037 ± 0.009

3.4. Mechanical characterization

Fig. 4 shows the dependence of the viscoelastic moduli (E' and E'') on frequency values from uniaxial tension tests (Fig. 4A) as well as the tensile stress-strain curve (Fig. 4B) obtained for the system containing BSA (10 wt%) and HPMC (3 wt%). Fig. 4A evidences the predominant solid-like behavior of the membranes developed by electrospinning, since the elastic modulus is much higher than the viscous one, reaching 10 MPa, and both moduli show a low dependence of the viscoelastic moduli on frequency. The elastic-dominant response is confirmed by the low values achieved for the loss tangent, ranging from 0.047 to 0.058. Similar results were reported for PVA-based electrospun nanofiber mats [75]. The values obtained are in the same order of magnitude than protein-based injection molded materials, but much lower than those obtained for commercial synthetic polymers such as LDPE [76]. As for the stress-strain curve, Fig. 4B shows an initial linear elastic behavior marked by a constant stress-strain slope, followed by limited plastic deformation. At the end of this plastic deformation stage, the probe breaks down. The initial slope determines the Young's Modulus (E), whereas the maximum value reach determines the maximum stress (σ_{max}) and the strain where the probe breaks down is the strain at break (ε_{max}). These values were 1.1 ± 0.1 MPa, 0.53 MPa and 0.85% for E, σ_{max} and ε_{max}, respectively. This value of E is lower than those reported for PVA electrospun nanofiber mats which typically range from 30 to 50 MPa [77–79]. However, it coincides with the values reported for cellulose acetate mats [80], being lower than those reported by Stylianopoulos et al. [81], who found an apparent dependence of the E value on the concentration for the polymer solution subjected to the electrospinning process. The value of the maximum stress is also lower than those found for other polymer electrospun mats. Thus, σ_{max} typically ranges for PVA from 2.5 to 8.5·MPa [78,79,82]. A value of ca. 5 MPa was also found for the ultimate tensile stress of EC/HPMC electrospun nanofiber mats [83]. In any case, the results obtained in this study confirm reasonably good mechanical strength for the BSA/HPMC membranes, which are also characterized by the limited deformation

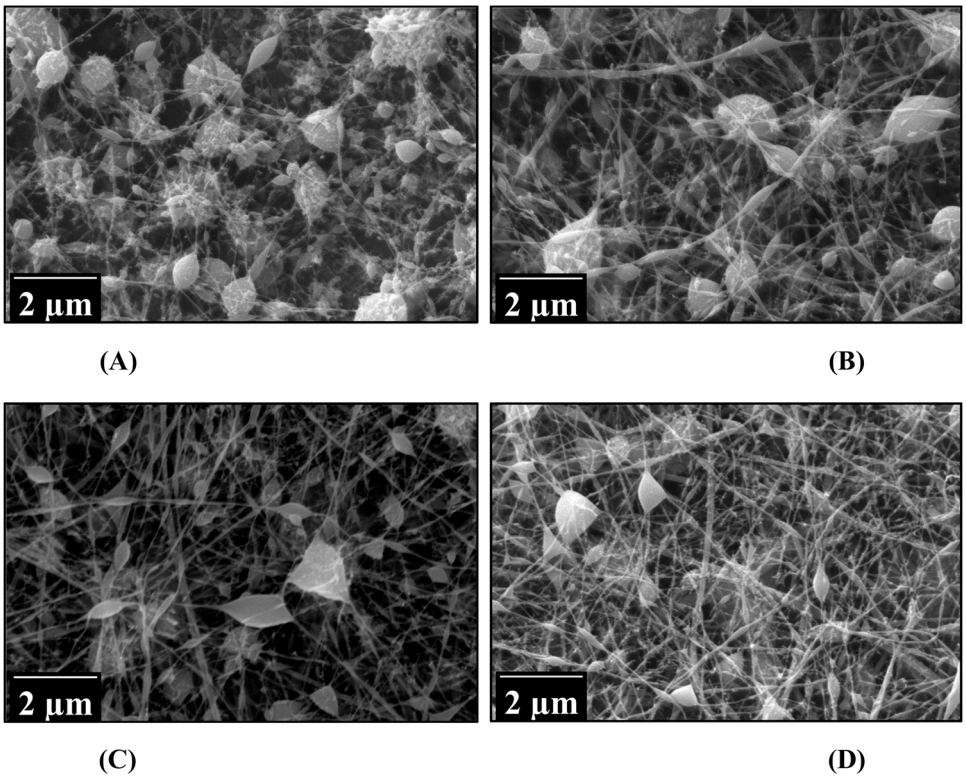

Fig. 2. Micrographs of the mats at 10 wt% BSA and HPMC as additive; **(A)** 1.5 wt% HPMC; **(B)** 2 wt% HPMC; **(C)** 2.5 wt% HPMC; **(D)** 3 wt% HPMC.

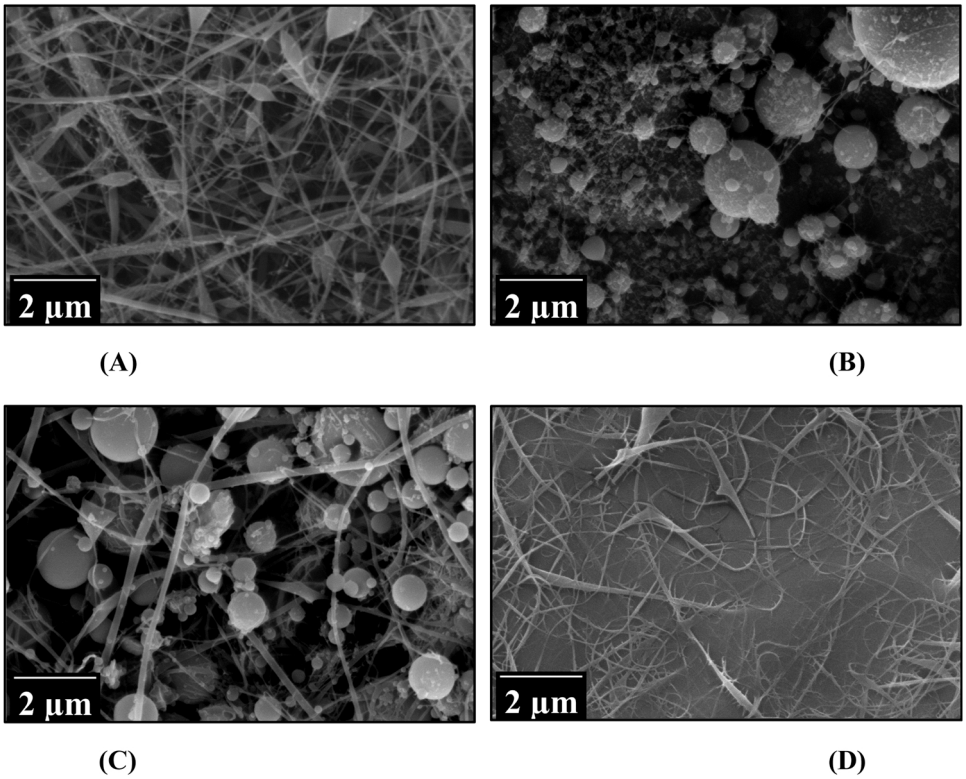

Fig. 3. Micrographs of the mats with different concentrations of BSA and HPMC, with Tween-20, SDS and NaCl as additives: **(A)** 10 wt% BSA + 3 wt% HPMC + 0.006 mM Tween-20; **(B)** 10 wt% BSA + 3 wt% HPMC + 0.1 wt% SDS; **(C)** 10 wt% BSA + 3 wt% HPMC + 15 mM NaCl; **(D)** 3 wt% HPMC.

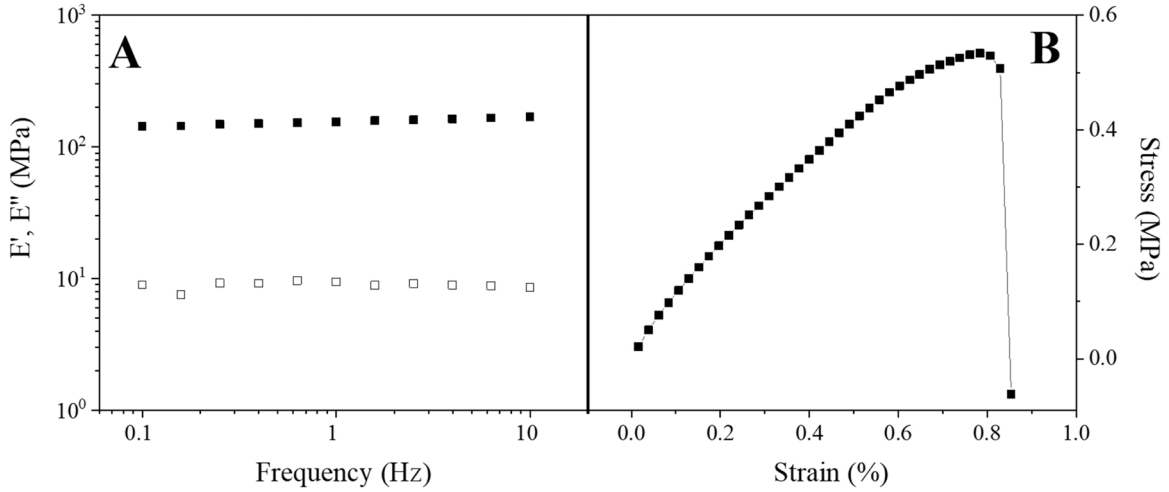

Fig. 4. Mechanical spectra (A) and the stress-strain curve obtained for the BSA (10 wt%) and HPMC (3 wt%) solution.

before breakage.

4. Conclusions

The results obtained indicated that electrospinning of BSA-based mats can be used to obtain diverse morphologies (from spherical particles to fibers) depending on the applied conditions. The use of SDS and β-ME led to structural changes in the BSA that did not seem to enhance the formation of nanofibers since they did not produce major changes in viscosity. Ethanol favored the formation of nanoparticles (~ 300 nm) obtained by electrosprying. Thermal denaturation of BSA led to a great increase in viscosity due to its gelation. G' increased from 0.1 to 80 Pa (for 89:11 and 80:20 H_2O:EtOH ratio, respectively) when the samples were heated up to 60 ºC. The formation of a crosslinked network in this sample might have hindered the processing of nanofiber-based membranes.

Co-electrospinning of BSA with HPMC was successfully achieved, which eventually led to nanofibrous mats (with fibers diameters of ca. 60 nm). BSA was successfully spread throughout the fibers in the resulting membranes, although it tended to accumulate in beads (the N content increased from 14 ± 2–21 ± 2% when fibers and beads are compared). HPMC served as structural support for BSA in these fibers, while BSA brought charges into the solution and disrupted the network formed by the HPMC molecules, favoring the solvent evaporation. Higher HPMC concentrations induced higher viscosities, which resulted in a lower concentration of beads. Moreover, the addition of non-ionic surfactant (Tween-20) enhanced bead removal. Additives exert a critical influence on the structure formed by the HPMC network and BSA molecules. So that, the addition of NaCl and SDS promoted the formation of nanoparticles rather than nanofibers.

Therefore, these results concluded that it is possible to achieve the electrospinning of membranes with advanced properties by using only biopolymers such as BSA and HPMC, where the protein exerts a crucial role.

CRediT authorship contribution statement

Javier Garcia: Investigation, Writing – original draft. **Manuel Felix**: Investigation, Methodology, Experiments, Data acquisition, Writing – review & editing. **Felipe Cordobes**: Validation, Formal analysis, Supervision. **Antonio Guerrero**: Supervision, Formal analysis, Funding acquisition.

Declaration of Competing Interest

The authors declare that they have no known competing financial interests or personal relationships that could have appeared to influence the work reported in this paper.

Data availability

Data will be made available on request.

Acknowledgments

The authors would like to thank Spanish "Ministerio de Ciencia e Innovación (MCI)/Agencia Estatal de Investigación (AEI)/Fondo Europeo de Desarrollo Regional (FEDER, UE)" for the financial support provided through the funding of the RTI2018-097100-B-C21 (MCI/AEI/FEDER, UE) project. Moreover, the authors also acknowledge the University of Seville (Spain) for the VPPI-US grant (Ref.-II.5) to Manuel Felix and the CITIUS service (from University of Seville, Spain) for granting access to and their assistance with the Microscopy service.

Appendix A. Supporting information

Supplementary data associated with this article can be found in the online version at doi:10.1016/j.colsurfb.2022.112683.

References

[1] Y. Ding, H. Hou, Y. Zhao, Z. Zhu, H. Fong, Electrospun polyimide nanofibers and their applications, Prog. Polym. Sci. 61 (2016) 67–103, https://doi.org/10.1016/j.progpolymsci.2016.06.006.
[2] F.-L. Zhou, R.-H. Gong, Manufacturing technologies of polymeric nanofibres and nanofibre yarns, Polym. Int. 57 (2008) 837–845, https://doi.org/10.1002/pi.2395.
[3] S. Castro Coelho, B. Nogueiro Estevinho, F. Rocha, Encapsulation in food industry with emerging electrohydrodynamic techniques: Electrospinning and electrospraying – a review, Food Chem. 339 (2021), 127850, https://doi.org/10.1016/j.foodchem.2020.127850.
[4] T. Kowalczyk, A. Nowicka, E. Danek, K. Tomasz A, Electrospinning of bovine serum albumin. Optimization and the use for production of biosensors, Biomacromolecules (2008) 2087–2090.
[5] Y. Liu, M. Hao, Z. Chen, L. Liu, Y. Liu, W. Yang, S. Ramakrishna, A review on recent advances in application of electrospun nanofiber materials as biosensors (2020). doi:10.1016/j.cobme.2020.02.001.
[6] K.S. Rho, L. Jeong, G. Lee, B.M. Seo, Y.J. Park, S.D. Hong, S. Roh, J.J. Cho, W. H. Park, B.M. Min, Electrospinning of collagen nanofibers: effects on the behavior of normal human keratinocytes and early-stage wound healing, Biomaterials 27 (2006) 1452–1461, https://doi.org/10.1016/j.biomaterials.2005.08.004.
[7] J.P. Ye, J.S. Gong, C. Su, Y.G. Liu, M. Jiang, H. Pan, R.Y. Li, Y. Geng, Z.H. Xu, J. S. Shi, Fabrication and characterization of high molecular keratin based nanofibrous membranes for wound healing, Colloid Surf. B 194 (2020), 111158, https://doi.org/10.1016/j.colsurfb.2020.111158.

[8] Z. Chen, X. Mo, F. Qing, Electrospinning of collagen–chitosan complex, Mater. Lett. 61 (2007) 3490–3494, https://doi.org/10.1016/j.matlet.2006.11.104.
[9] A.M.M. Sousa, H.K.S. Souza, J. Uknalis, S.-C. Liu, M.P. Gonçalves, L. Liu, Electrospinning of agar/PVA aqueous solutions and its relation with rheological properties, Carbohydr. Polym. 115 (2015) 348–355, https://doi.org/10.1016/j.carbpol.2014.08.074.
[10] A. Koski, K. Yim, S. Shivkumar, Effect of molecular weight on fibrous PVA produced by electrospinning, Mater. Lett. 58 (2004) 493–497, https://doi.org/10.1016/S0167-577X(03)00532-9.
[11] Y. Li, H. Yuan, Y. Chen, X. Wei, K. Sui, Y. Tan, Application and exploration of nanofibrous strategy in electrode design, J. Mater. Sci. Technol. 74 (2021) 189–202, https://doi.org/10.1016/j.jmst.2020.10.015.
[12] M.C. McManus, E.D. Boland, H.P. Koo, C.P. Barnes, K.J. Pawlowski, G.E. Wnek, D. G. Simpson, G.L. Bowlin, Mechanical properties of electrospun fibrinogen structures, Acta Biomater. 2 (2006) 19–28, https://doi.org/10.1016/j.actbio.2005.09.008.
[13] L. Wannatong, A. Sirivat, P. Supaphol, Effects of solvents on electrospun polymeric fibers: preliminary study on polystyrene, Polym. Int. 53 (2004) 1851–1859, https://doi.org/10.1002/pi.1599.
[14] W.E. Teo, S. Ramakrishna, A review on electrospinning design and nanofibre assemblies, Nanotechnology 17 (2006) R89, https://doi.org/10.1088/0957-4484/17/14/R01.
[15] N. Bhardwaj, S.C. Kundu, Electrospinning: a fascinating fiber fabrication technique, Biotechnol. Adv. 28 (2010) 325–347, https://doi.org/10.1016/j.biotechadv.2010.01.004.
[16] S.K. Tiwari, S.S. Venkatraman, Importance of viscosity parameters in electrospinning: of monolithic and core–shell fibers, Mater. Sci. Eng. C 32 (2012) 1037–1042, https://doi.org/10.1016/j.msec.2012.02.019.
[17] S. Ramakrishna, An Introduction to Electrospinning and Nanofibers, World Scientific, 2005.
[18] Q. Yang, L.I. Zhenyu, Y. Hong, Y. Zhao, S. Qiu, C.E. Wang, Y. Wei, Influence of solvents on the formation of ultrathin uniform poly(vinyl pyrrolidone) nanofibers with electrospinning, J. Polym. Sci. Part B Polym. Phys. 42 (2004) 3721–3726, https://doi.org/10.1002/polb.20222.
[19] N. Amariei, L.R. Manea, A.P. Bertea, A. Bertea, A. Popa, The influence of polymer solution on the properties of electrospun 3D nanostructures, IOP Conf. Ser. Mater. Sci. Eng. 209 (2017), https://doi.org/10.1088/1757-899X/209/1/012092.
[20] R. Khajavi, M. Abbasipour, Controlling Nanofiber Morphology by the Electrospinning Process, Elsevier Ltd, 2017, https://doi.org/10.1016/B978-0-08-100907-9.00005-2.
[21] S.K. Boda, X. Li, J. Xie, Electrospraying an enabling technology for pharmaceutical and biomedical applications: a review, J. Aerosol Sci. 125 (2018) 164–181, https://doi.org/10.1016/j.jaerosci.2018.04.002.
[22] G. Eda, J. Liu, S. Shivkumar, Solvent effects on jet evolution during electrospinning of semi-dilute polystyrene solutions, Eur. Polym. J. 43 (2007) 1154–1167, https://doi.org/10.1016/j.eurpolymj.2007.01.003.
[23] G. Tetteh, A.S. Khan, R.M. Delaine-Smith, G.C. Reilly, I.U. Rehman, Electrospun polyurethane/hydroxyapatite bioactive Scaffolds for bone tissue engineering: The role of solvent and hydroxyapatite particles, J. Mech. Behav. Biomed. Mater. 39 (2014) 95–110, https://doi.org/10.1016/j.jmbbm.2014.06.019.
[24] T. Jarusuwannapoom, W. Hongrojjanawiwat, S. Jitjaicham, L. Wannatong, M. Nithitanakul, C. Pattamaprom, P. Koombhongse, R. Rangkupan, P. Supaphol, Effect of solvents on electro-spinnability of polystyrene solutions and morphological appearance of resulting electrospun polystyrene fibers, Eur. Polym. J. 41 (2005) 409–421, https://doi.org/10.1016/j.eurpolymj.2004.10.010.
[25] K. Nasouri, A.M. Shoushtari, M.R.M. Mojtahedi, Effects of polymer/solvent systems on electrospun polyvinylpyrrolidone nanofiber morphology and diameter, Polym. Sci. Ser. A 57 (2015) 747–755, https://doi.org/10.1134/S0965545X15060164.
[26] C.J. Luo, M. Nangrejo, M. Edirisinghe, A novel method of selecting solvents for polymer electrospinning, Polymer 51 (2010) 1654–1662, https://doi.org/10.1016/j.polymer.2010.01.031.
[27] J.W. Sissons, A. Nyrup, P.J. Kilshaw, R.H. Smith, Ethanol denaturation of soya bean protein antigens, J. Sci. Food Agric. 33 (1982) 706–710.
[28] C. Tanford, in: C.B. Anfinsen, J.T. Edsall, F.M. Richards (Eds.), Protein Denaturation: Part C, Academic Press, 1970, pp. 1–95, https://doi.org/10.1016/S0065-3233(08)60241-7.
[29] M.L. Anson, A.E. Mirsky, The effect of denaturation on the viscosity of protein systems, J. Gen. Physiol. 15 (1932) 341–350, https://doi.org/10.1085/jgp.15.3.341.
[30] K.C. Bauer, S. Suhm, A.K. Wöll, J. Hubbuch, Impact of additives on the formation of protein aggregates and viscosity in concentrated protein solutions, Int. J. Pharm. 516 (2017) 82–90, https://doi.org/10.1016/j.ijpharm.2016.11.009.
[31] N. O'Brien, A. McKee, D.C. Sherrington, A.T. Slark, A. Titterton, Facile, versatile and cost effective route to branched vinyl polymers, Polymer 41 (2000) 6027–6031, https://doi.org/10.1016/S0032-3861(00)00016-1.
[32] X. Li, Y. Peng, Y. Deng, F. Ye, C. Zhang, X. Hu, Y. Liu, D. Zhang, Recycling and reutilizing polymer waste via electrospun micro/nanofibers: a review, Nanomaterials 12 (2022), https://doi.org/10.3390/nano12101663.
[33] I.N. Strain, Q. Wu, A.M. Pourrahimi, M.S. Hedenqvist, R.T. Olsson, R.L. Andersson, Electrospinning of recycled PET to generate tough mesomorphic fibre membranes for smoke filtration, J. Mater. Chem. A 3 (2015) 1632–1640, https://doi.org/10.1039/C4TA06191H.
[34] S.P. Zhong, W.E. Teo, X. Zhu, R.W. Beuerman, S. Ramakrishna, L.Y.L. Yung, An aligned nanofibrous collagen scaffold by electrospinning and its effects on in vitro fibroblast culture, J. Biomed. Mater. Res. Part A 79A (2006) 456–463, https://doi.org/10.1002/jbm.a.30870.
[35] F. Muneer, M.S. Hedenqvist, S. Hall, R. Kuktaite, Innovative green way to design biobased electrospun fibers from wheat gluten and these fibers' potential as absorbents of biofluids, ACS Environ. Au 2 (2022) 232–241, https://doi.org/10.1021/acsenvironau.1c00049.
[36] H. Homayoni, S.A.H. Ravandi, M. Valizadeh, Electrospinning of chitosan nanofibers: processing optimization, Carbohydr. Polym. 77 (2009) 656–661, https://doi.org/10.1016/j.carbpol.2009.02.008.
[37] S.O. Han, J.H. Youk, K.D. Min, Y.O. Kang, W.H. Park, Electrospinning of cellulose acetate nanofibers using a mixed solvent of acetic acid/water: effects of solvent composition on the fiber diameter, Mater. Lett. 62 (2008) 759–762, https://doi.org/10.1016/j.matlet.2007.06.059.
[38] A. Frenot, M.W. Henriksson, P. Walkenström, Electrospinning of cellulose-based nanofibers, J. Appl. Polym. Sci. 103 (2007) 1473–1482, https://doi.org/10.1002/app.24912.
[39] Y. Dror, T. Ziv, V. Makarov, H. Wolf, A. Admon, E. Zussman, Nanofibers made of globular proteins, Biomacromolecules 9 (2008) 2749–2754, https://doi.org/10.1021/bm8005243.
[40] D.L. Woerdeman, P. Ye, S. Shenoy, R.S. Parnas, G.E. Wnek, O. Trofimova, Electrospun fibers from wheat protein: Investigation of the interplay between molecular structure and the fluid dynamics of the electrospinning process, Biomacromolecules 6 (2005) 707–712, https://doi.org/10.1021/bm0494545.
[41] A.C. Mendes, K. Stephansen, I.S. Chronakis, Electrospinning of food proteins and polysaccharides, Food Hydrocoll. 68 (2017) 53–68, https://doi.org/10.1016/j.foodhyd.2016.10.022.
[42] J.D. Schiffman, C.L. Schauer, A review: electrospinning of biopolymer nanofibers and their applications, Polym. Rev. 48 (2008) 317–352, https://doi.org/10.1080/15583720802022182.
[43] D.B. Khadka, D.T. Haynie, Protein- and peptide-based electrospun nanofibers in medical biomaterials, Nanomed. Nanotechnol. Biol. Med. 8 (2012) 1242–1262, https://doi.org/10.1016/j.nano.2012.02.013.
[44] D.L. Woerdeman, S. Shenoy, D. Breger, Role of chain entanglements in the electrospinning of wheat protein-poly(vinyl alcohol) blends, J. Adhes. 83 (2007) 785–798, https://doi.org/10.1080/00218460701588398.
[45] A.A. Moosavi-Movahedi, Thermodynamics of protein denaturation by sodium dodecyl sulfate, J. Iran. Chem. Soc. 2 (2005) 189–196, https://doi.org/10.1007/BF03245921.
[46] P.G. Righetti, G. Tudor, E. Gianazza, Effect of 2-mercaptoethanol on pH gradients in isoelectric focusing, J. Biochem. Biophys. Methods 6 (1982) 219–227, https://doi.org/10.1016/0165-022X(82)90044-6.
[47] A. Nikolaidis, T. Moschakis, On the reversibility of ethanol-induced whey protein denaturation, Food Hydrocoll. 84 (2018) 389–395, https://doi.org/10.1016/j.foodhyd.2018.05.051.
[48] A. Teo, K.K.T. Goh, J. Wen, I. Oey, S. Ko, H.-S. Kwak, S.J. Lee, Physicochemical properties of whey protein, lactoferrin and Tween 20 stabilised nanoemulsions: effect of temperature, pH and salt, Food Chem. 197 (2016) 297–306, https://doi.org/10.1016/j.foodchem.2015.10.086.
[49] C.X. Zhang, X.Y. Yuan, L.L. Wu, Y. Han, J. Sheng, Study on morphology of electrospun poly(vinyl alcohol) mats, Eur. Polym. J. 41 (2005) 423–432, https://doi.org/10.1016/j.europolymj.2004.10.027.
[50] B. Kim, H. Park, S.-H. Lee, W.M. Sigmund, Poly(acrylic acid) nanofibers by electrospinning, Mater. Lett. 59 (2005) 829–832, https://doi.org/10.1016/j.matlet.2004.11.032.
[51] A.H. Hunt, B. Jirgensons, Effect of sodium dodecyl sulfate and its homologs on circular dichroism of α-chymotrypsin, Biochemistry 12 (1973) 4435–4441, https://doi.org/10.1021/bi00746a021.
[52] L. Yong, H. Ji-Huan, Y. Jian-yong, Z. Hong-mei, Controlling numbers and sizes of beads in electrospun nanofiber, Polym. Int. 57 (2008) 632–636, https://doi.org/10.1002/pi.
[53] A. Aydogdu, G. Sumnu, S. Sahin, A novel electrospun hydroxypropyl methylcellulose/polyethylene oxide blend nanofibers: morphology and physicochemical properties, Carbohydr. Polym. 181 (2018) 234–246, https://doi.org/10.1016/j.carbpol.2017.10.071.
[54] S.B. Barbuddhe, J. Vergis, D.B. Rawool, Chapter 4 - Immunodetection of bacteria causing brucellosis, in: C.S. Pavia, V.B.T.-M. in M. Gurtler (Eds.), Immunological Methods in Microbiology, Academic Press, 2020, pp. 75–115. doi:https://doi.org/10.1016/bs.mim.2019.11.003.
[55] M.M. Nielsen, K.K. Andersen, P. Westh, D.E. Otzen, Unfolding of β-sheet proteins in SDS, Biophys. J. 92 (2007) 3674–3685, https://doi.org/10.1529/biophysj.106.101238.
[56] S.F. Santos, D. Zanette, H. Fischer, R. Itri, A systematic study of bovine serum albumin (BSA) and sodium dodecyl sulfate (SDS) interactions by surface tension and small angle X-ray scattering, J. Colloid Interface Sci. 262 (2003) 400–408, https://doi.org/10.1016/S0021-9797(03)00109-7.
[57] F. Herná Inz-Bermú Dez De Castro, A. Gá Lvez-Borrego, Surface tension of aqueous solutions of sodium dodecyl sulfate from 20 °C to 50 °C and pH between 4 and 12, 1998.
[58] A. Abutaleb, D. Lolla, A. Aljuhani, H.U. Shin, J.W. Rajala, G.G. Chase, Effects of surfactants on the morphology and properties of electrospun polyetherimide fibers, Fibers 5 (2017) 1–14, https://doi.org/10.3390/fib5030033.
[59] F. Yalcinkaya, B. Yalcinkaya, O. Jirsak, Dependent and independent parameters of needleless electrospinning, Vlakna Text. 2015 (2015) 75–79, https://doi.org/10.5772/65838.
[60] C.J. Angammana, S.H. Jayaram, Analysis of the effects of solution conductivity on electrospinning process and fiber morphology, IEEE Trans. Ind. Appl. 47 (2011) 1109–1117, https://doi.org/10.1109/TIA.2011.2127431.

[61] S. Huan, G. Liu, G. Han, W. Cheng, Z. Fu, Q. Wu, Q. Wang, Effect of experimental parameters on morphological, mechanical and hydrophobic properties of electrospun polystyrene fibers, Materials 8 (2015) 2718–2734, https://doi.org/10.3390/ma8052718.
[62] R.M. Nezarati, M.B. Eifert, E. Cosgriff-Hernandez, Effects of humidity and solution viscosity on electrospun fiber morphology, (n.d.). doi:10.1089/ten.tec.2012.0671.
[63] O. Regev, S. Vandebril, E. Zussman, C. Clasen, The role of interfacial viscoelasticity in the stabilization of an electrospun jet, Polymer 51 (2010) 2611–2620, https://doi.org/10.1016/j.polymer.2010.03.061.
[64] T.J. Sill, H.A. von Recum, Electrospinning: applications in drug delivery and tissue engineering, Biomaterials 29 (2008) 1989–2006, https://doi.org/10.1016/j.biomaterials.2008.01.011.
[65] K. Takeda, A. Wada, K. Yamamoto, Y. Moriyama, K. Aoki, Conformational change of bovine serum albumin by heat treatment, J. Protein Chem. 8 (1989) 653–659, https://doi.org/10.1007/BF01025605.
[66] V.S. Devi, O.O. Chidi, D. Coleman, Dominant effect of ethanol in thermal destabilization of bovine serum albumin in the presence of sucrose, Spectroscopy 23 (2009) 265–270, https://doi.org/10.3233/SPE-2009-0400.
[67] M. Félix, C. Carrera, A. Romero, C. Bengoechea, A. Guerrero, C. Carrera-Sanchez, A. Romero, C. Bengoechea, A. Guerrero, Rheological approaches as a tool for the development and stability behaviour of protein-stabilized emulsions, Food Hydrocoll. 104 (2020), 105719, https://doi.org/10.1016/j.foodhyd.2020.105719.
[68] O.E. Pérez, C. Carrera-Sánchez, J.M. Rodríguez-Patino, A.M.R. Pilosof, Adsorption dynamics and surface activity at equilibrium of whey proteins and hydroxypropyl–methyl–cellulose mixtures at the air-water interface, Food Hydrocoll. 21 (2007) 794–803, https://doi.org/10.1016/j.foodhyd.2006.11.013.
[69] J.-C. Arboleya, P.J. Wilde, Competitive adsorption of proteins with methylcellulose and hydroxypropyl methylcellulose, Food Hydrocoll. 19 (2005) 485–491, https://doi.org/10.1016/j.foodhyd.2004.10.013.
[70] N. Chandran, C. Sarathchandran, S. Thomas, Introduction to Rheology, Elsevier Inc, 2019, https://doi.org/10.1016/B978-0-12-816957-5.00001-X.
[71] J. Schurz, Rheology of polymer solutions of the network type, Prog. Polym. Sci. 16 (1991) 1–53, https://doi.org/10.1016/0079-6700(91)90006-7.
[72] S. Choi, J.K. Park, Microfluidic rheometer for characterization of protein unfolding and aggregation in microflows, Small 6 (2010) 1306–1310, https://doi.org/10.1002/SMLL.201000210.
[73] A. Srivastava, A. Prajapati, Albumin and functionalized albumin nanoparticles: production strategies, characterization, and target indications, Asian Biomed. 14 (2020) 217–242, https://doi.org/10.1515/abm-2020-0032.
[74] N. Matsudomi, D. Rector, J.E. Kinsella, Gelation of bovine serum albumin and β-lactoglobulin; effects of pH, salts and thiol reagents, Food Chem. 40 (1991) 55–69, https://doi.org/10.1016/0308-8146(91)90019-K.
[75] M. Félix, C. Jiménez, A. Romero, A. Guerrero, PVA-based electrospun nanofiber mats of potential use in active packaging, Inte, J. Environ. Agric. Res. 2 (2016) 7–14.
[76] V. Perez-Puyana, M. Felix, A. Romero, A. Guerrero, Effect of the injection moulding processing conditions on the development of pea protein-based bioplastics, J. Appl. Polym. Sci. 133 (2016) 43306, https://doi.org/10.1002/app.43306.
[77] J. Li, J. Suo, R. Deng, Structure, mechanical, and swelling behaviors of poly (vinyl alcohol)/SiO2 hybrid membranes, J. Reinf. Plast. Compos. 29 (2010) 618–629.
[78] A. Rianjanu, A. Kusumaatmaja, E.A. Suyono, K. Triyana, Solvent vapor treatment improves mechanical strength of electrospun polyvinyl alcohol nanofibers, Heliyon 4 (2018), e00592, https://doi.org/10.1016/j.heliyon.2018.e00592.
[79] Y. Shi, Y. Zhao, X. Li, D. Yan, D. Cao, Z. Fu, Enhancement of the mechanical properties and thermostability of poly(vinyl alcohol) nanofibers by the incorporation of sodium chloride, J. Appl. Polym. Sci. 135 (2018) 45981, https://doi.org/10.1002/app.45981.
[80] Z. Ma, M. Kotaki, S. Ramakrishna, Electrospun cellulose nanofiber as affinity membrane, J. Membr. Sci. 265 (2005) 115–123, https://doi.org/10.1016/j.memsci.2005.04.044.
[81] T. Stylianopoulos, M. Kokonou, S. Michael, A. Tryfonos, C. Rebholz, A.D. Odysseos, C. Doumanidis, Tensile mechanical properties and hydraulic permeabilities of electrospun cellulose acetate fiber meshes, J. Biomed. Mater. Res. Part B Appl. Biomater. 100B (2012) 2222–2230, https://doi.org/10.1002/jbm.b.32791.
[82] K.Y. Lee, L. Jeong, Y.O. Kang, S.J. Lee, W.H. Park, Electrospinning of polysaccharides for regenerative medicine, Adv. Drug Deliv. Rev. 61 (2009) 1020–1032, https://doi.org/10.1016/j.addr.2009.07.006.
[83] L. Yavari, M. Ghorbani, A novel aloe vera-loaded ethylcellulose/hydroxypropyl methylcellulose nanofibrous mat designed for wound healing application, J. Polym. (2021), https://doi.org/10.21203/rs.3.rs-517639/v1.